SHEAR DEFORMATION OF REINFORCED CONCRETE BEAM

(Translation from Journal of Materials, Conc. Struct. Pavements, JSCE, No.711/V-56, August 2002)

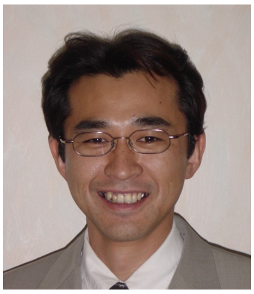

Tamon UEDA Yasuhiko SATO Tsunemasa ITO Katsuhide NISHIZONE

This paper presents the experimental results on shear deformation of concrete beams with shear reinforcement, which was measured by laser speckle method. The results indicate that, besides flexural deformation, a significant amount of shear deformation occurs after shear cracking, as a result of localized shear deformation along shear cracks. Based on the experimental results, a rather simple mechanical model for prediction of the deformation is proposed. The model consists of a truss model that calculates the shear deformation and a modified Branson's model with the tension shift concept to calculate the flexural deformation. The model can predict the experimental results well.

Keywords: *reinforced concrete beam, shear deformation, truss model, flexural deformation*

UEDA Tamon is a professor in the Division of Structural and Geotechnical Engineering at Hokkaido University. He obtained D.Eng. from the University of Tokyo in 1982. His research interests widely cover mechanics of reinforced concrete, steel-concrete composite and continuous fiber reinforced concrete structures. He is a member of JSCE.

Yasuhiko SATO is a research associate in the Division of Structural and Geotechnical Engineering at Hokkaido University, Sapporo, Japan. He obtained his D.Eng. from Hokkaido University in 1994. His research interests relate to development of design and analytical methods for newly constructed, existing and strengthened concrete members under cyclic actions. He is a member of JSCE.

Tsunemasa ITO is a subsection chief in the Facilities and Rolling Stock Division of Railway Bureau at Ministry of Land, Infrastructure and Transport, Tokyo, Japan. He obtained his M.Eng. from Hokkaido University in 1998. He is a member of JSCE.

Katsuhide NISHIZONE is a special assistant to the director of the Environment and Engineering Division at Ports and Harbors Bureau, Ministry of Land, Infrastructure and Transport, Tokyo, Japan. He obtained his M.Eng. from Hokkaido University in 1995. He is a member of JSCE.

1. INTRODUCTION

Recently accurate prediction of deformations of reinforced concrete members has been considered more important because the performance-based design will be introduced as the next generation of design of structures. The performance-based design clearly specifies what are required performances of structures for serviceability, many of which are related to deformations of structures.

It is well known that flexural deformations of concrete members can be calculated with reasonable accuracy by the Branson's equation [1], which is based on the Euler's beam theory. At the same time it is known that the Euler's theory, assuming that a plane in a beam remains after its flexural deformation, is no longer applicable after shear cracking [2]; in such cases, the neutral axis depth after shear cracking is smaller than predicted by the Euler's beam theory.

It is considered that after shear cracking shear deformation is no longer negligible. However, there is no method commonly accepted for prediction of shear deformation. The truss theory, which is often used for predictions of shear strength and shear reinforcement stress, has seldom been used for the prediction of deformation. One reason for the lack of a method for evaluating shear deformation seems to be the difficulty in measurement of shear deformation in experiments.

In this study, the laser speckle method is applied to measure shear deformation of beams with shear reinforcement. Based on the experimental results, a rather simple model to calculate deformation of beams is proposed. This model consists of a truss model for calculating shear deformation and a modified Branson's model for calculating flexural deformation. In the truss model tension stiffness of concrete surrounding shear reinforcement is considered. The influence of tension force increment in tension reinforcement induced by truss action after shear cracking, which is conventionally called moment shift, is considered in calculation of flexural deformation. In this paper, "moment shift" is called "tension shift".

2. OUTLINE OF EXPERIMENT

The experimental specimens consisted of four small and one large beams with shear reinforcement. The experimental parameters are shear span to effective depth ratio, tension reinforcement ratio, and shear reinforcement ratio. Details of the specimens are given in **Fig.1** and **Table 1**. Specimens No.1-4 are the small beams. Specimens No.2, 3, and 4 are identical to specimen No.1, the reference beam, except for shear span to effective depth ratio (or effective depth), tension reinforcement ratio, and shear reinforcement ratio, respectively. Specimen No.5 is the large beam. The concrete strength for each specimen is shown in **Table 1**. The maximum aggregate size was 15 mm. Young's modulus and the strength of tension and shear reinforcement are shown in **Table 2**. High strength tension reinforcement was chosen for specimen No.3, so as to ensure that flexural yielding would not occur.

Deflection at the loading point was measured using displacement transducer for all the specimens and at additional three points in shear span for specimen No.5 (see **Fig.1 (c)**). Shear deformation in shear span in the small specimens (specimens No.1-4) was measured by the laser speckle method [3]. The laser speckle method is an optical measurement method for in-plane displacement.

Movement in any direction of any point within a target area can be measured with an accuracy of 1 μm order using the laser speckle method. The size of the target area depends on the specifications of the laser; in this test the area was approximately 300×300 mm, and this was the reason why shear span was chosen to be 300 mm for the small specimens. The movements of sixty-six nodes (fifty-five nodes for specimen No.2) shown in **Fig.2** were measured by the laser speckle method to calculate strains, ε_x, ε_y and γ_{xy} of 100 triangle elements (80 elements for specimen No.2). The strains of the upper triangles were calculated using the nodal movements u and v as follows:

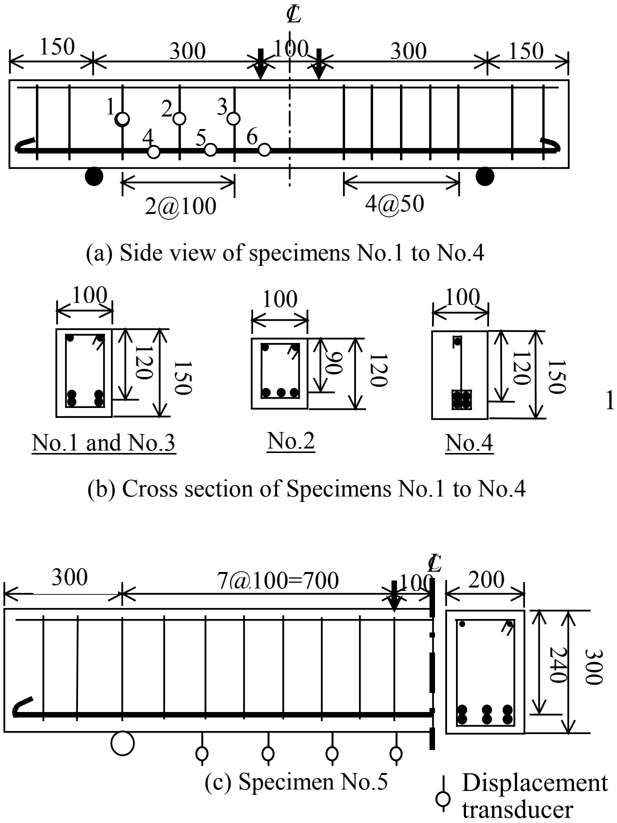

Fig.1 Specimens

$$\varepsilon_x = (u_j - u_i)/\Delta x \tag{1a}$$

$$\varepsilon_y = (v_k - v_i)/\Delta y \tag{1b}$$

$$\gamma_{xy} = (u_k - u_i)/\Delta x + (v_j - v_i)/\Delta y \tag{1c}$$

An explanation of the notation used here is given in **Fig.3**. Strains for the lower triangles can be calculated in a similar way. The location of the neutral axis was obtained from distribution of ε_y. The shear deformation of the specimen, δ_s, was calculated as the average shear strain in the shear span multiplied by the shear span length, a, as follows:

$$\delta_s = \bar{\gamma}_{xy} a = \frac{\gamma_{xy1} + \gamma_{xy2}}{2} a \tag{2}$$

where $\gamma_{xy1} = (u_2 - u_1)/h + (v_4 - v_1)/a$ (3a)

$$\gamma_{xy2} = -(u_4 - u_3)/h - (v_2 - v_3)/a \tag{3b}$$

Table 1 Specimens and test results

Specimen	f'_c (MPa)	a/d	p_s (%)	p_w (%)	V_u (kN)
No.1	40.2	2.5	4.22	0.63	67
No.2	54.7	3.3	4.22	0.63	39
No.3	41.0	2.5	2.38	0.63	60
No.4	40.5	2.5	4.22	0.32	48
No.5	31.7	2.92	4.46	0.72	235

1) f'_c : concrete strength, a/d : shear span to depth ratio, p_s : tension reinforcement ratio, p_w : shear reinforcement ratio, and V_u : ultimate strength

Table 2 Material properties of reinforcement

Type	A_s (mm^2)	f_y (MPa)	E_s (GPa)
D6	31.67	355	183
D10	71.33	791	197
D13	126.7	355	170
D22	387.1	392	178

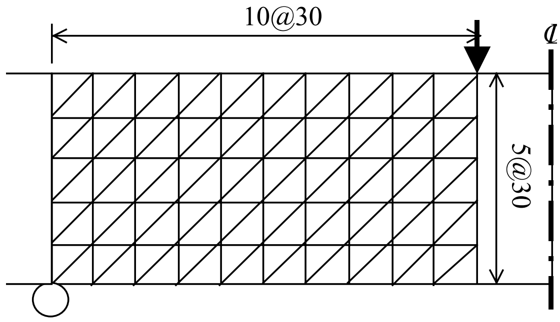

Fig.2 Measuring points for laser speckle method (specimens No.1, 3, and 4)

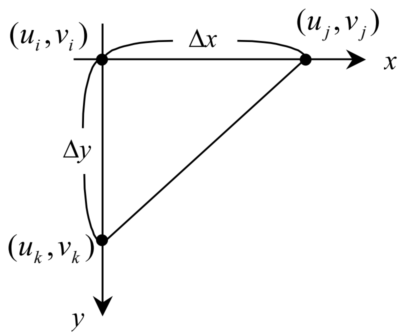

Fig.3 Grid for calculation of strain

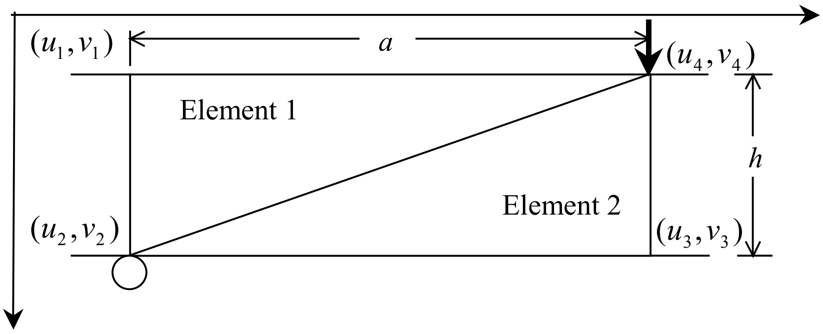

Fig.4 Calculation of shear deformation

The notation used here is explained in **Fig.4**. The flexural deformation of the specimen, δ_f, was calculated by subtracting the shear deformation from the deflection at the loading point, δ, namely:

$$\delta_f = \delta - \delta_s \tag{4}$$

Strains of the tension reinforcement were measured at maximum moment region and at points between shear reinforcement (see **Fig.1 (a)**). Strains were measured at one point of each shear reinforcement in the small specimens and at two points of each shear reinforcement in the large specimen.

The load was monotonically increased with a displacement increment of 200 μm at the loading point until the specimens failed.

3. EXPERIMENTAL RESULTS

3.1 Failure characteristics

Specimen No.1 failed in flexure with yielding of the tension reinforcement, while all other specimens showed shear failure without yielding of the tension reinforcement.

3.2 Deformation characteristics

The relationship between applied shear force and deflection at the loading point in specimen No.2 is shown in **Fig.5**. It is seen that deflection at the loading point up to onset of shear cracking can be predicted using the following equation derived from the Euler's beam theory in which the Branson's equation for effective moment of inertia is applied:

$$\delta_f = \frac{Va^3}{6E_c I_e}\left\{-x^3 + 3a(a+2c)x\right\} \tag{5}$$

where V is the applied shear force, E_c is Young's modulus of concrete, x is the distance from support to the point considered ($0 \le x \le a$), a is the shear span, c is half of the distance between two loading points, and I_e is the effective moment of inertia that can be calculated as follows:

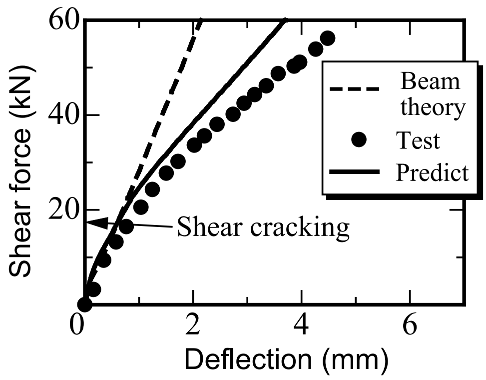

Fig.5 Relationship between applied shear force and total deformation

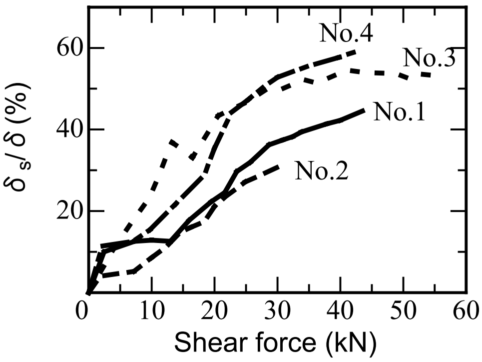

Fig.6 Ratio of shear deformation to total deformation

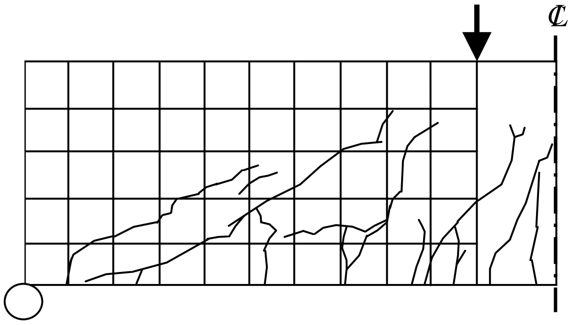

Fig.7 Cracking pattern in specimen No.1

$$I_e = I_g \left(\frac{M_{cr}}{M_{\max}} \right)^3 + I_{cr} \left\{ 1 - \left(\frac{M_{cr}}{M_{\max}} \right)^3 \right\} \qquad (6)$$

where I_g and I_{cr} are moment of inertia of concrete gross and cracked section, M_{cr} and $M_{\max}$ are cracking and maximum moment at loading point under applied shear force, V.

It can be said, therefore, that before shear cracking deformation is mostly flexural deformation. However, after shear cracking, the observed deflection is significantly greater than that calculated by the Branson's equation. Shear cracking clearly has an effect.

The ratio of shear deformation to total deformation (δ_s / δ) for the smaller specimen is shown in **Fig.6**. The shear deformation is calculated by Eq.(2). This ratio is larger for specimens with a smaller shear span to effective depth ratio, smaller tension reinforcement ratio, and smaller shear reinforcement ratio.

3.3 Concrete strain characteristics

Cracking pattern observed in specimen No.1 is shown in **Fig.7**. Its distribution of shear strain for specimen No.1, calculated as average of shear strains in a pair of upper and lower triangle elements (see **Figs. 2** and **3**), is shown in **Fig.8**. The corresponding distribution of principal strains is shown in **Fig.9**. It can be said that after shear cracking took place at 22 kN, large, localized shear strains appeared along the shear crack. The normal strain distribution in specimen No.1 is

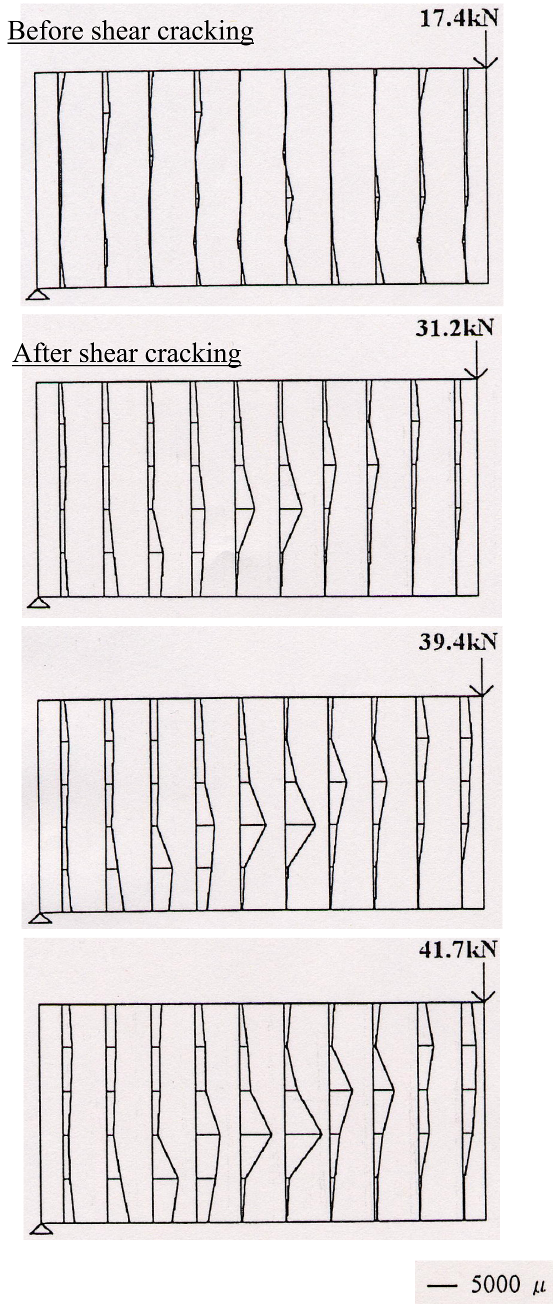

Fig.8 Concrete shear strain distribution

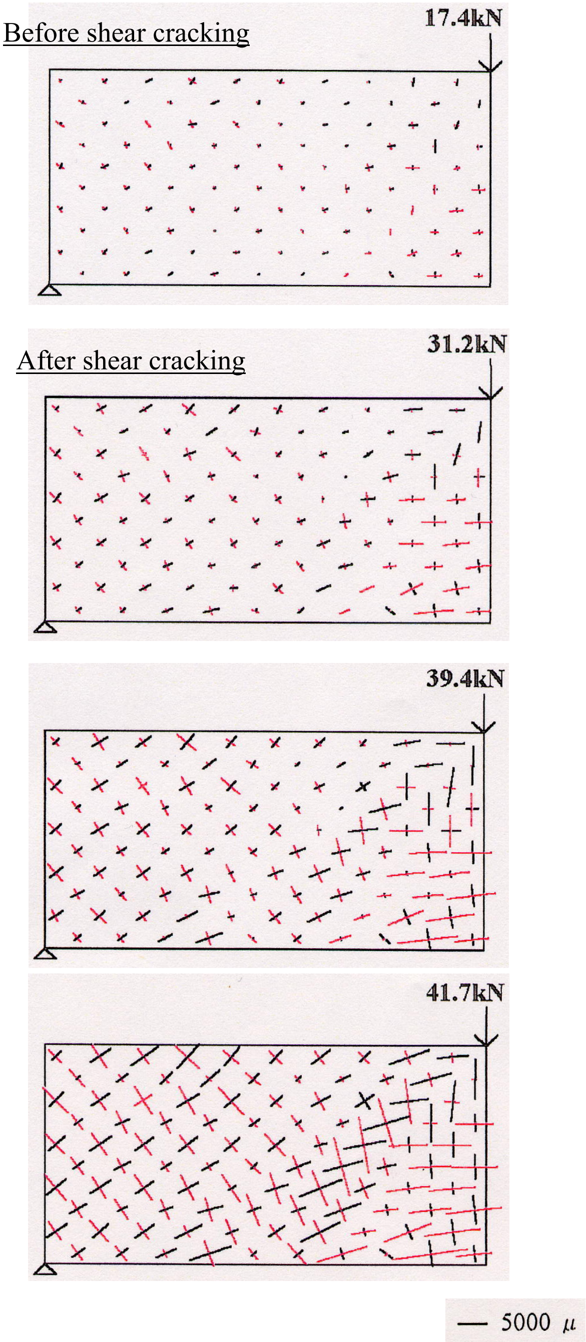

Fig.9 Principal strain distribution

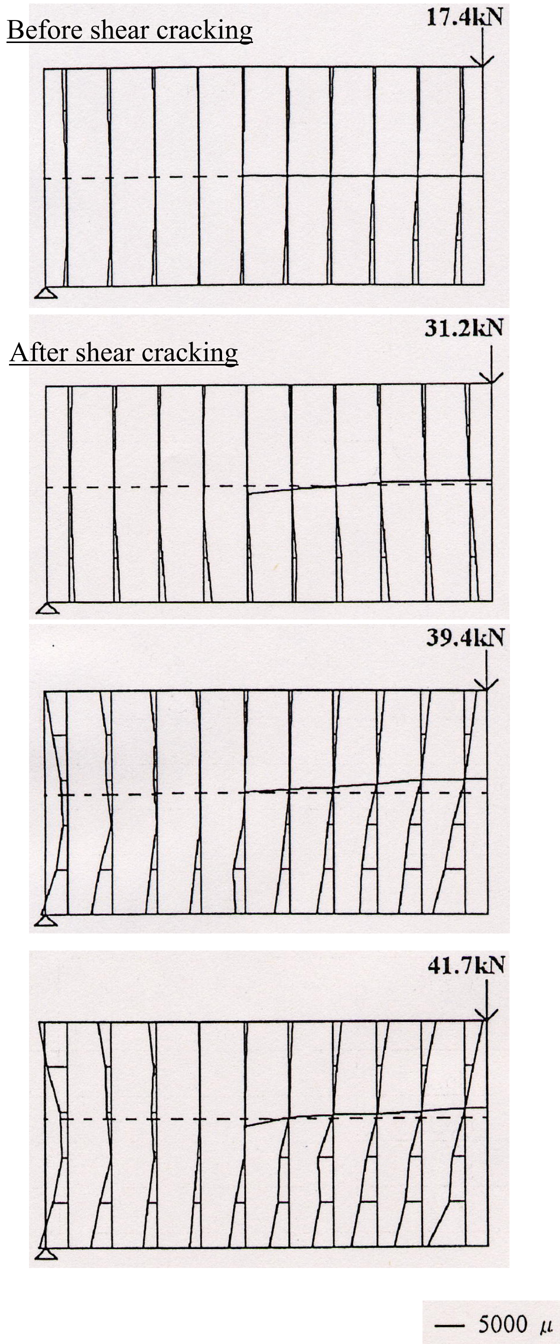

Fig.10 Normal strain in direction of member axis and neutral axis

indicated in **Fig.10**. It is clearly seen that the observed neutral axis depth (indicated by solid lines) is smaller than that predicted for an Euler beam with no concrete stress in tension (broken lines).

3.4 Reinforcement strain characteristics

The relationship between applied shear force and strain in the tension reinforcement for specimen No.4 is shown in **Fig.11**. The strain in the tension reinforcement at point 4 (see **Fig.1 (a)**) increases more quickly and becomes larger than the predicted by the Euler's beam theory with stiffness of cracked section. This quicker increase can be explained by so called "moment shift". Moment shift is explained by truss action in which horizontal component of force in diagonal compression strut is balanced with force in tension chord (tension reinforcement). Since diagonal strut does not exist in beam action, additional force would act in tension reinforcement once truss action begins acting.

The shear reinforcement strain of specimen No.3 is shown as with respect to applied shear force in **Fig.12**. The measuring point was point 3 in **Fig.1 (a)**. It is known that the relationship between applied shear force, V, and shear reinforcement strain, ε_w, can be expressed by truss action as follows:

$$V = V_c + V_s = V_c + A_w E_w \varepsilon_w \left(\cot\alpha + \cot\theta\right) z/s \tag{7}$$

where V_c is the applied shear force at shear cracking, V_s is the shear force carried by truss mechanism, A_w is the cross sectional area of the shear reinforcement within spacing, s, E_w and α are Young's modulus of shear reinforcement and its angle to the member axis, θ is the angle of compression diagonal strut, and z is the distance between centroids of forces in the compression and tension chords. The observed strain in **Fig.12** is much smaller than that predicted by Eq.(7).

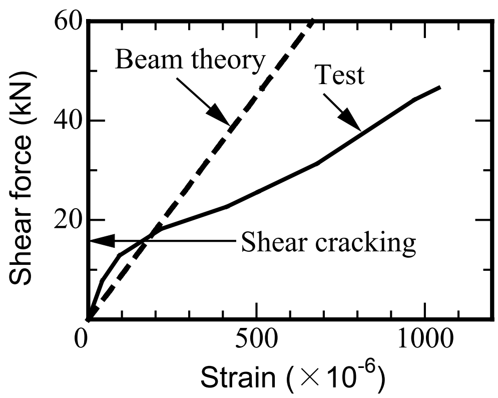

Fig.11 Relationship between applied shear force and strain in tension reinforcement

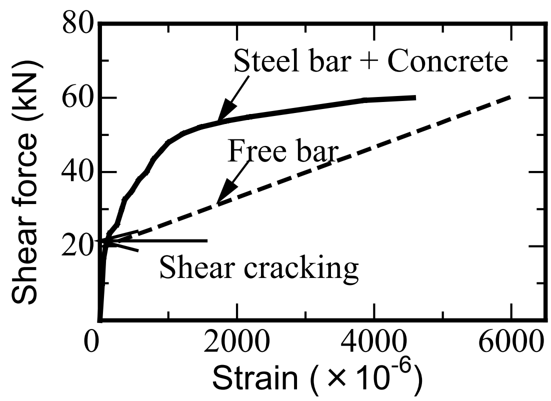

Fig.12 Relationship between applied shear force and strain in shear reinforcement

4. PROPOSED MODEL FOR SHEAR DEFORMATION

In this section proposed model for calculation of shear deformation before and after flexural and shear cracking of beams is presented. Shear deformation includes additional flexural deformation due to shear cracking.

4.1 Model for additional flexural deformation due to shear cracking

It is considered that the Branson's method can be used to calculate flexural deformation with consideration of tension force increase in tension reinforcement induced by truss action occurring after shear cracking (see **Fig.11**). Since this is actually a change in tension force in the tension reinforcement rather than a change in the moment acting on the beam, the new terminology, "tension shift" will be adapted in this study instead of the conventional "moment shift".

The amount of the tension shift, ΔT, can be calculated from truss mechanism, which carries part of the total shear force, V_s. For this purpose, a free body of the truss mechanism is considered as shown in **Fig.13**. Line *CD* is parallel to the diagonal compression strut whose angle to the member axis is θ.

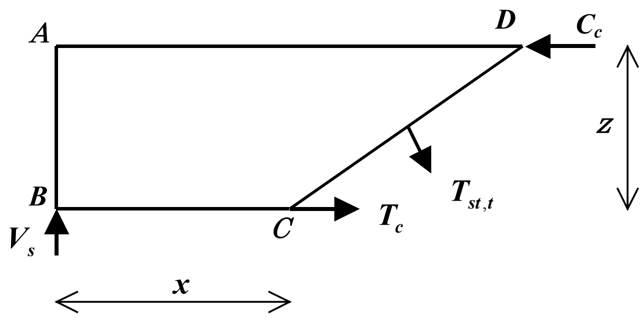

Fig. 13 Free body for calculation of tension shift, ΔT

From the equilibrium of tension forces across the line *CD*, $T_{st,t}$ and V_s, the following equation is derived:

$$T_{st,t} = \frac{V_s}{\sin\alpha} \tag{8}$$

where α is the angle of the shear reinforcement to the member axis. The equilibrium of moments around point *D* induced by tension forces acting in the tension chord, T_c, $T_{st,t}$ and V_s is,

$$V_s(x + z\cot\theta) - T_c z - \frac{1}{2}\frac{z}{\sin\theta}\sin(\theta+\alpha)T_{st,t} = 0 \tag{9}$$

where x is the distance of point *C* from the support. Substituting Eq.(8) in Eq.(9), the following equation is then obtained:

$$T_c = \left[\frac{x}{z} + \cot\theta - \frac{\sin(\theta+\alpha)}{2\sin\theta\sin\alpha}\right]V_s \tag{10}$$

If it is assumed that beam action carries the total shear force subtracted by the shear force carried by the truss mechanism, $V - V_s$, the tension force in the tension reinforcement (or the tension chord in truss) at point *C* is

$$T_b = \frac{x}{z}(V - V_s) \tag{11}$$

On the other hand, if beam action carries all the shear force, tension force in the tension reinforcement at point *C* is

$$T = \frac{x}{z}V \tag{12}$$

From Eqs.(10), (11), and (12), the amount of tension shift, ΔT, that is the tension force increase in the tension reinforcement is as follows:

$$\Delta T = T_c + T_b - T = \left[\cot\theta - \frac{\sin(\theta+\alpha)}{2\sin\theta\sin\alpha}\right]V_s \tag{13}$$

However, the total tension force in tension reinforcement never goes beyond the maximum tension force induced by moment. Additional flexural deformation due to the tension shift is calculated by assuming that the tension shift creates additional deformation whose amount is the same as that caused by moment inducing the same amount of tension force in tension reinforcement. This assumption is in fact conservative. The reason is as follows. Actually additional deformation due to increase in moment in beam action is different from that due to tension shift in truss mechanism. The moment increase causes increase in elongation in tension zone and contraction in compression zone, while the tension shift increases elongation in both tension and compression chords of the truss mechanism. The elongation of the tension chord is much greater than that of the compression chord because the tension chord is cracked concrete (or tension reinforcement) and the compression chord is uncracked concrete. This difference in elongation induces additional flexural deformation, which is smaller than that induced by an increase in the moment in beam action.

4.2 Model for shear deformation before shear cracking

It is assumed that shear deformation before shear cracking can be calculated by elastic theory for beam as follows:

$$\delta_s = \kappa \int \frac{V}{G_c A_e} dx \tag{14}$$

where $\kappa = 6/5$ a for rectangular section, G_c is the shear stiffness of concrete ($= E_c/[2(1+\nu_c)]$), ν_c is Poisson's ratio of concrete, and A_e is the concrete effective cross-sectional area, which is calculated as follows:

before flexural cracking,

$$A_e = A_g \tag{15a}$$

after flexural cracking,

$$A_e = A_g \left(\frac{M_{cr}}{M_{\max}} \right)^3 + A_{cr} \left[1 - \left(\frac{M_{cr}}{M_{\max}} \right)^3 \right] \tag{15b}$$

where A_g is the concrete gross section ($= bh$ for a rectangular section), b and h are the width and height of the cross section, n is the ratio of Young's modulus ($= E_s/E_c$) and A_{cr} is the cross-sectional area of the cracked section. Equation (15b) is introduced under the assumption that the effective concrete area for shear stiffness is reduced due to flexural cracking.

Although Eqs.(14) and (15) are proposed here, experimental facts indicate that shear deformation is usually much smaller than flexural deformation and can be neglected.

4.3 Shear deformation after shear cracking

After shear cracking, it is assumed that shear deformation is caused by truss mechanism. Since deformation of truss due to deformation of tension and compression chord is considered in flexural deformation, truss deformation due to deformation of tie and compression strut is considered as shear deformation. Let's consider a truss unit $ABCD$ consisting of tie and compression strut horizontal extent of $z(\cot\theta + \cot\alpha)$ and vertical size of z, as shown in **Fig.14**. The truss unit is a part of a beam where shear cracks exist. Line BE is parallel to the compression strut whose angle to tension chord (or tension reinforcement) is θ. Line CE is parallel to tie whose angle is α. The cross-sectional area of the compression strut crossing line CE is as follows:

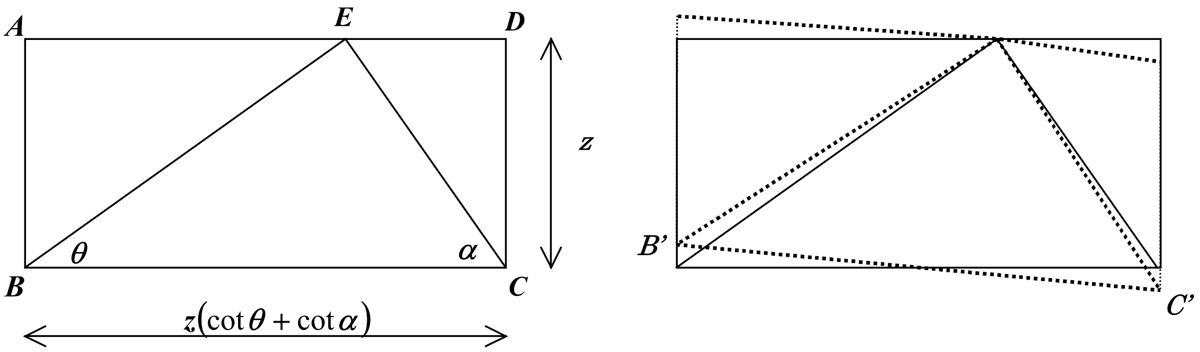

(a) Assumed truss unit (b) Deformation of truss unit

Fig.14 Truss unit for calculation of shear deformation

$$A_{st,c} = b_w z(\cot\theta + \cot\alpha)\sin\theta \tag{16}$$

When applied shear force on the truss mechanism is V_s, stress acting in compression strut is calculated under equilibrium as follows:

$$\sigma'_{st,c} = \frac{V_s}{A_{st,c}\sin\theta} = \frac{V_s}{b_w z(\cot\theta + \cot\alpha)\sin^2\theta} \tag{17}$$

Thus the strain in compression strut is

$$\varepsilon'_{st,c} = \frac{\sigma'_{st,c}}{E_c} \tag{18}$$

Since the length of compression strut is

$$l_{st,c} = \frac{z}{\sin\theta} \tag{19}$$

The deformation (shortening) of the compression strut is

$$\Delta l_{st,c} = l_{st,c}\varepsilon'_{st,c} = \frac{V_s}{E_c b_w(\cot\theta + \cot\alpha)\sin^3\theta} \tag{20}$$

This deformation moves point B to B' in **Fig.14**. The vertical component of the movement of point B that indicates shear deformation induced by deformation of compression strut is expressed by the following equation:

$$\delta_{s1} = \frac{\Delta l_{st,c}}{\sin\theta} = \frac{V_s}{E_c b_w(\cot\theta + \cot\alpha)\sin^4\theta} \tag{21}$$

Similarly, the shear deformation due to deformation of the tie can be calculated. The cross-sectional area of the tie, consisting of the shear reinforcement and the surrounding concrete effective in tension, is assumed to be

$$A_{st,to} = A_w + \frac{E_c}{E_w} A_{ce} \tag{22}$$

with $$A_{ce} = A_{ceo} \left(V_c / V \right)^3 \tag{23}$$

where A_w is the cross-sectional area of the shear reinforcement in a spacing, s, A_{ce} is cross-sectional area of the surrounding concrete effective in tension, and A_{ceo} is A_{ce} immediate after shear cracking and can be calculated using the method proposed by An et al [5]. The number of shear reinforcement crossing line BE is

$$n_w = \frac{z(\cot\theta + \cot\alpha)}{s} \tag{24}$$

The cross-sectional area of the tie, crossing line BE is

$$A_{st,t} = \frac{z(\cot\theta + \cot\alpha)}{s} \left(A_w + \frac{E_c}{E_w} A_{ce} \right) \tag{25}$$

The stress in the tie can be calculated by equilibrium as follows:

$$\sigma_{st,t} = \frac{V_s}{A_{st,t} \sin\alpha} = \frac{V_s s}{\left(A_w + \frac{E_c}{E_w} A_{ce} \right) z(\cot\theta + \cot\alpha)\sin\alpha} \tag{26}$$

The strain in the tie is then

$$\varepsilon_{st,t} = \frac{\sigma_{st,t}}{E_w} \tag{27}$$

Since the length of the tie is

$$l_{st,t} = \frac{z}{\sin\alpha} \tag{28}$$

The deformation (elongation) of the tie is

$$\Delta l_{st,t} = l_{st,t} \varepsilon_{st,t} = \frac{V_s s}{E_w \left(A_w + \frac{E_c}{E_w} A_{ce} \right) (\cot\theta + \cot\alpha)\sin^2\alpha} \tag{29}$$

Due to this deformation, point C moves to C' in **Fig.14**. Vertical component of the movement, which is a part of shear deformation, is expressed by the following equation:

$$\delta_{s2} = \frac{\Delta l_{st,t}}{\sin\alpha} = \frac{V_s s}{E_w\left(A_w + \frac{E_c}{E_w}A_{ce}\right)(\cot\theta + \cot\alpha)\sin^3\alpha} \tag{30}$$

Consequently, the shear deformation of the truss unit shown in **Fig.14** can be calculated from Eqs.(21) and (30) as follows:

$$\delta_s = \delta_{s1} + \delta_{s2} \tag{31}$$

Its corresponding shear strain is

$$\gamma = \frac{\delta_s}{z(\cot\theta + \cot\alpha)} \tag{32}$$

Finally, the shear deformation of the beam can be calculated by integrating the shear strain as follows:

$$\delta_s = \int \gamma dx = \int \frac{1}{z(\cot\theta + \cot\alpha)^2}\left[\frac{V_s}{E_c b_w \sin^4\theta} + \frac{V_s s}{E_w\left(A_w + \frac{E_c}{E_w}A_{ce}\right)\sin^3\alpha}\right]dx \tag{33}$$

The angle of the tie, α, is given as the angle of the shear reinforcement to the member axis. However, the compression strut angle, θ, has to be given based on actual compression stress flow in the concrete. In this study numerical experiment with nonlinear finite element program [4] was conducted to find θ. **Figure 15** shows the variation of θ, which was found to increase slightly before shear cracking and decrease gradually after shear cracking. It was also found that the variation of θ was influenced by some factors such as shear span to depth ratio, tension reinforcement ratio and shear reinforcement ratio. As a result, the following equation is proposed to evaluate the θ variation with reasonable accuracy (see **Fig.15**):

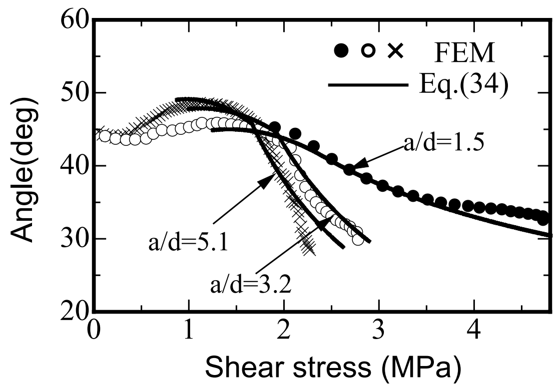

Fig.15 Angle of compression strut

$$\theta = -\alpha(v - v_0)^2 + \theta_0 \quad \text{for} \quad v_0 \le v < 1.7v_c \tag{34a}$$

$$\theta = \theta_1\left(\frac{1.7v_0}{v}\right)^\beta \quad \text{for} \quad 1.7v_c \le v \tag{34b}$$

with $\theta_0 = 3.2\left(\frac{a}{d}\right) + 40.2$ for $a/d > 1.5$ (35)

$$\theta_1 = -\alpha(1.7v_c - v_0)^2 + \theta_0 \quad (36)$$

$$v_0 = 0.9v_c \quad (37)$$

$$v_c = 0.2 f_c'^{1/3}(100p_t)^{1/3}(1/d)^{1/4}\left(0.75 + \frac{1.4}{a/d}\right) \quad (38)$$

$$\alpha = 0.4\left(\frac{a}{d}\right)^2 + 2.9 \quad (39)$$

$$\beta = (0.7 - 32\sqrt{p_t p_w})\frac{a}{d} \quad (40)$$

where v is nominal shear stress $(= V/(bd))$, v_c is nominal shear stress at shear cracking, p_t is tension reinforcement ratio, p_w is shear reinforcement ratio, and a/d is shear span to depth ratio (>1.5).

Consequently shear deformation after shear cracking is a summation of the shear deformation of the truss calculated by Eq.(33) and the shear deformation immediately before shear cracking calculated by Eq.(36).

$$\delta_{sc} = k\int \frac{V_c}{GA_e}dx \quad (41)$$

Because of its nature, Eq.(33) for calculation of shear deformation can be applied to not only the case of point loading but also distributed loading. In the latter case the shear force carried by the truss mechanism, V_s or $V - V_c$ varies with different x.

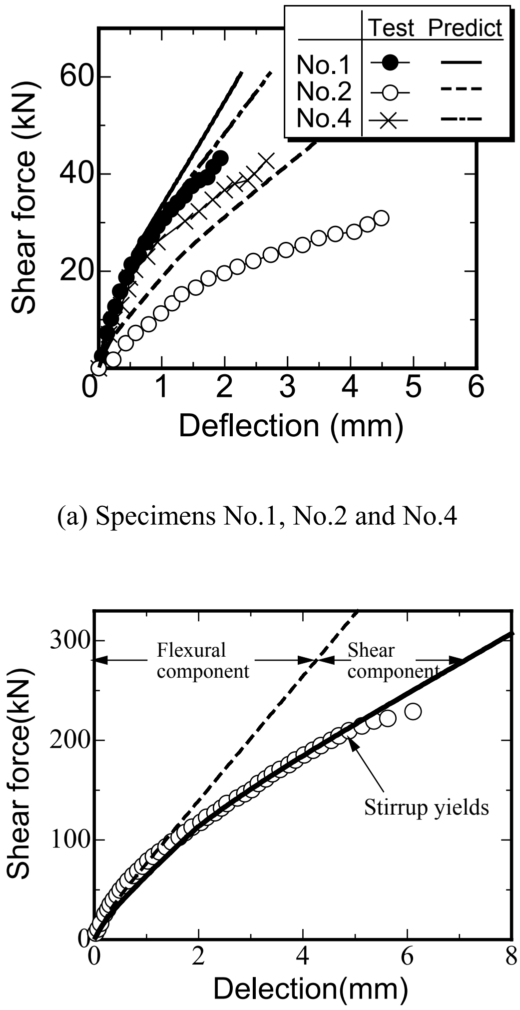

(a) Specimens No.1, No.2 and No.4

(b) Specimen No.5

Fig.16 Comparison of predicted deformation with observed deformation

4.4 Verification of proposed model

Figure 16 shows comparison between experimental and calculated load-deformation curves of specimens No.1, No.2, No.4 and No.5. A result of specimen No.3 is shown in **Fig.5**. As seen in **Fig.16(b)** the calculated flexural deformation significantly underestimates the experimental deformation after shear cracking. The proposed model can simulate the experimental results reasonably for specimens No.1, No.3 and No.5. In specimen No.2 the observed deformation is larger than calculated one from the early stage because displacement at supporting points could not be measured correctly. It could be considered in specimen No.4 that slippage of stirrup at the hook (see **Fig.1**) have produced the unexpected deformation.

Figure 17 shows comparison with previous study [6] in which the tension and shear reinforcement ratios, and *a*/*d* are varied from 1.8 to 3.7%, 0.8 to 2%, and 3.92 to 6.98, respectively (see **Table 3**). It can be said that the proposed model can predict the experimental results with good accuracy except for higher load level

Table 3 Test specimens in Ref.(6)

Specimen	f'_c (MPa)	a/d	p_s (%)	p_w (%)
A-1	24	3.92	1.8	1.0
A-2	24	4.93	2.3	1.0
A-3	35	6.91	2.7	1.0
B-1	25	3.95	2.4	0.8
B-2	23	4.91	2.4	1.5
B-3	39	6.95	3.1	1.5
C-1	30	3.95	1.8	2.0
C-2	24	4.93	3.7	2.0
C-3	35	6.98	3.6	2.0

in some specimen with smaller *a/d* ratios. The discrepancy in the higher load level observed in specimens A-1, A-2, B-1, and B-2 may be caused by yielding of stirrups. Unfortunately no information on the yielding is given in the reference.

The proposed model will be extended to the model which can consider the yielding of reinforcing bars.

5. CONCLUSIONS

(1)The two-dimensional distribution of shear strain in a shear span was measured by an optical measuring method (the laser speckle method). It was observed that shear strain was rather localized along the shear crack.
(2)Significant shear deformation was observed after shear cracking in the experiment.
(3)Due to the shear deformation the conventional method for prediction of flexural deformation (Branson's method) underestimates the observed deformation significantly.
(4)Methods to calculate additional flexural deformation due to tension shift induced by shear cracking and to calculate shear deformation were presented.
(5)This prediction method for shear deformation that is based on truss mechanism can be applied to not only point loading but also distributed loading.
(6)The proposed methods predict the observed deformation with reasonable accuracy.

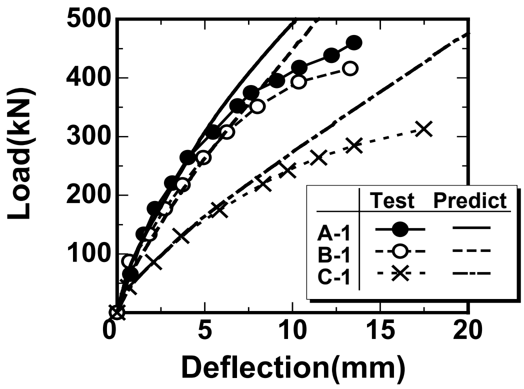

(a) *a*/*d* is about 4.0

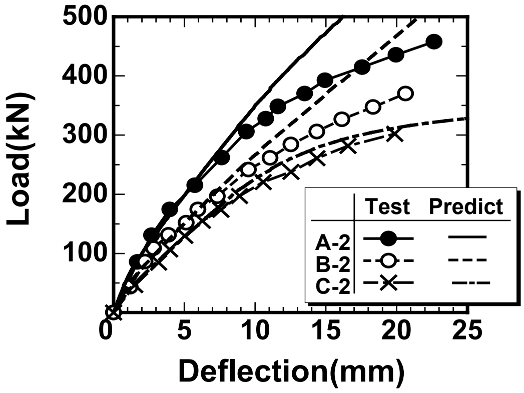

(b) *a*/*d* is about 5.0

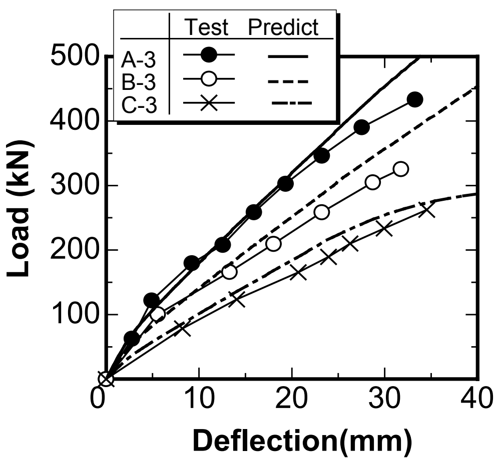

(c) *a*/*d* is about 7.0

Fig.17 Comparison with experimental results reported in Ref.(6)

Acknowledgment

The authors would like to express their gratitude to Prof. KAKUTA Yoshio and Prof.TAKAHASHI Yoshihiro for their valuable advice related to this study and to Mr. KIMURA Tsutomu for his assistance to the experiments.

References

[1]Branson. D. E. and Trost, H.: Unified procedures for predicting the deformation and centroidal axis location of partially cracked nonprestressed and prestressed concrete members, *ACI J.*, Vol.79, No.2, pp.119-128, 1982.
[2]Sato, Y., Ueda, T. and Kakuta, Y.: Qualitative evaluation of shear resisting behavior of concrete beams reinforced with FRP rods by finite element analysis", *Concrete Library International*, JSCE, No.24, pp.193-209, 1994.
[3]Pallewatta. T. M., Tada, H. and Horii, H.: Measurement of displacement field of concrete by laser speckle method, *Transactions of JCI*, Vol.12, No.1, pp.835-840, 1990.
[4]Ueda, T., Pantaratorn, N. and Sato, Y.: Finite element analysis on shear resisting mechanism of concrete beams with shear reinforcement", *Journal of Materials, Concrete Structures and Pavements*, JSCE, No.520／V-28, pp.273-286, 1995.
[5]An, X., Maekawa, and K., Okamura, H.: Numerical simulation of size effect in shear strength of RC beams, *Concrete Library of JSCE*, NO. 31, pp. 323-346, 1998.
[6]Clark, A. P., Diagonal tension in reinforced concrete beams, *ACI J.*, Vol.23, No.2, pp.145-156, 1951.